

Practical Robust Localization over Large-Scale 802.11 Wireless Networks

Andreas Haeberlen
Rice University
ahae@cs.rice.edu

Eliot Flannery
Rice University
ef@cs.rice.edu

Andrew M. Ladd
Rice University
aladd@cs.rice.edu

Algis Rudys
Rice University
arudys@cs.rice.edu

Dan S. Wallach
Rice University
dwallach@cs.rice.edu

Lydia E. Kavraki
Rice University
kavraki@cs.rice.edu

ABSTRACT

We demonstrate a system built using probabilistic techniques that allows for remarkably accurate localization across our entire office building using nothing more than the built-in signal intensity meter supplied by standard 802.11 cards. While prior systems have required significant investments of human labor to build a detailed signal map, we can train our system by spending less than one minute per office or region, walking around with a laptop and recording the observed signal intensities of our building's unmodified base stations. We actually collected over two minutes of data per office or region, about 28 man-hours of effort. Using less than half of this data to train the localizer, we can localize a user to the precise, correct location in over 95% of our attempts, across the entire building. Even in the most pathological cases, we almost never localize a user any more distant than to the neighboring office. A user can obtain this level of accuracy with only two or three signal intensity measurements, allowing for a high frame rate of localization results. Furthermore, with a brief calibration period, our system can be adapted to work with previously unknown user hardware. We present results demonstrating the robustness of our system against a variety of untrained time-varying phenomena, including the presence or absence of people in the building across the day. Our system is sufficiently robust to enable a variety of location-aware applications without requiring special-purpose hardware or complicated training and calibration procedures.

Categories and Subject Descriptors

C.2.1 [Computer Systems Organization]: Network Architecture and Design—*Wireless communication*; G.3 [Mathematics of Computing]: Probability and Statistics—*Markov processes, Probabilistic algorithms*; I.2.9 [Computing Methodologies]: Robotics—*Sensors*; I.5.1 [Pattern Recognition]: Models—*Statistical*

Permission to make digital or hard copies of all or part of this work for personal or classroom use is granted without fee provided that copies are not made or distributed for profit or commercial advantage and that copies bear this notice and the full citation on the first page. To copy otherwise, to republish, to post on servers or to redistribute to lists, requires prior specific permission and/or a fee.

MobiCom'04, Sept. 26-Oct. 1, 2004, Philadelphia, Pennsylvania, USA.
Copyright 2004 ACM 1-58113-868-7/04/0009 ...\$5.00.

General Terms

Algorithms, Design, Experimentation, Measurement

Keywords

802.11, wireless networks, mobile systems, topological localization, Bayesian methods, location-aware computing

1. INTRODUCTION

A practical scheme for mobile device location awareness has long been a target of mobility research. Many interesting applications, including systems like EasyLiving [6] and the Rhino Project [1], among others [2,13,14,35], would benefit from a practical location-sensing system. Until now, however, indoor location-sensing systems have either required specialized hardware, involved lengthy training steps, or had poor precision. A practical scheme should have relatively low training time, achieve high accuracy, use widely-deployed off-the-shelf hardware, and be robust in the face of untrained variations.

Most previous indoor location-sensing schemes have been based on occupancy grid models of the environment. Such schemes divide the environment into a coordinate grid, with one to two meter precision, and attempt to map a device's location to a point on that grid. Occupancy grid systems require lengthy training at each point in the grid to achieve usable accuracy.

Many location-aware applications, however, do not need one to two meter precision for the location of a mobile device. We use a topological model of our environment, in which the building is divided into cells which each map to a region in our building (i.e., a specific office or a hallway segment), and we map a device's location to a cell instead of a point. In this way, we trade off some metric resolution for a dramatic reduction in training time.

Room- or region-level granularity of location provides sufficient context for many location-aware applications. Additionally, operating at a coarser granularity leads to an improvement in localization robustness, and allows localization to occur with fewer samples, and thus operate at a higher frame rate.

We present a high-precision topological location inference technique based on Bayesian inference and using the 802.11 wireless network protocol. Most significant in our work is the scale. We deployed our wireless location-sensing system in our entire office building, which is over 12,000 square meters in area. Our technique can localize a device to one of 510 cells in the building within

seconds; it succeeded in over 95% of all attempts. When the localization is off, it is almost always off by only one cell (e.g., it thinks you are in the adjacent office). A training time of around 60 seconds per room is sufficient; thus, a small team can measure an entire office building in an evening. Our techniques are robust even against time-of-day variation, including the presence or absence or large groups of people in the same room as the platform being localized. Furthermore, our techniques allow us to calibrate and use 802.11 implementations different from the system used to initially measure the building. Our system supports both static localization and dynamic tracking at speeds of over 3 m/s.

We describe our basic localization system and report its performance in Section 2. Our analysis and experimental results on time-varying phenomena are presented in Section 3. Section 4 presents our calibration technique, which is designed to compensate for variations in hardware and time-varying phenomena. We discuss our results in Section 5 and present our conclusions in Section 6.

1.1 Related work

Location-aware computing [10,22] is primarily concerned with determining the location of a mobile computing device. Early in-building location-sensing systems required specialized hardware to ascertain a device’s location. For example, the Active Badge system relied on specialized tags which emitted diffuse infrared pulses detected by ceiling-mounted sensors [55]. The later Active Bat system used ultrasound time-of-flight information [56]. The Cricket Compass [40, 41] used specialized ultrasound and radio frequency receivers to detect signals transmitted by fixed beacons. In Spot-On [23], specialized wireless devices use signal intensity to localize either against fixed base stations or against one another in an ad-hoc fashion. Finally, EasyLiving [28] uses cameras to determine location.

Later systems for location-aware computing used off-the-shelf wireless networking hardware, measuring radio frequency signal intensity to determine the location of a mobile computing device. RADAR [4, 5] was one of the first systems to use RF signal intensity for location-sensing. Small et al. [46] and Smailagic et al. [45] looked at how signal intensity varies over time and developed a location-sensing system based on these observations. Gwon et al. [20] discuss two deterministic schemes for aggregating and improving the output of a location-sensing system.

The most recent systems have used probabilistic techniques for sensing a device’s location. Nibble [9], one of the first systems of this generation, used a neural network to estimate a device’s location. In our first work on wireless location sensing [31], we developed a grid-based Bayesian location-sensing system over a small region of our office building, achieving localization and tracking to within 1.5 meters over 50% of the time. Roos et al. [43] implemented a similar system and got similar localization results. They are also the first to compare taking a Gaussian fit of signal strength to using the full histogram of signal strength, although they came to no definite conclusion on this. In a follow-up to our previous work [31], we explored variations in hardware and transmission power, and addressed the symmetry of localizing a laptop by measuring the signal intensity of packets transmitted from a mobile device as received by a base station versus packets transmitted by a base station and received by the device [48]. Clustering techniques have also been applied to the problem of location determination [58]. Krumm and Platt [29] introduced a number of techniques for simplifying the process of training a location-sensing system, including localizing based on topological regions (e.g. rooms) rather than grid coordinates. Finally, Ekahau, Inc. [16] offer a wireless location-sensing system commercially; they claim

1 meter accuracy with a short training time, although they do not detail how their system works.

A number of localization techniques have been developed for other wireless technologies. For instance, in part as a result of the FCC’s E911 initiative [17], a number of systems have used RF signal intensity to determine the location of cellular phones [33, 57]. However, in the field of outdoor location-sensing, GPS [34] is still the standard.

Wireless localization techniques have also been explored for localization in sensor networks. Sensor networks are ad hoc networks of many autonomous nodes deployed to perform a variety of distributed sensing tasks [24,27,39]. Some techniques use signal properties, including signal strength [21], difference in time-of-arrival for RF versus ultrasound signals [44] and angle of arrival [37], to determine the physical location of sensor nodes. Other techniques use such factors as what nodes are in range [7] and routing information [36,38] to localize sensor nodes relative to one-another. Sequential Monte Carlo localization [25] utilizes the movement of sensor nodes to get improved accuracy of localization.

Wireless location-sensing is actually a specialized case of a well-studied problem in mobile robotics, that of robot localization — determining the position of a mobile robot given input from the robot’s various sensors (possibly including GPS, sonar, vision, and ultrasound sensors). Robot localization has been described as the most fundamental problem of building autonomous robots [12]. Our system and others like it use the signal intensity readings from 802.11 cards as a sensor and implement Bayesian localization algorithms commonly used in various robotics applications [8, 15, 19, 49]. Thrun [49] provides a comprehensive survey of probabilistic localization methods used in mobile robotics.

Our system creates a topological map for localization. A topological map models the environment as a graph, with each node representing a region (such as a particular room or corridor), and each edge representing regions that are connected in space. Remolina and Kuipers [42] present a comprehensive formal theory of topological mapping. Most work on topological mapping was originally explored as a means of building a map of an environment while simultaneously localizing within that map [11,30,50,51,54].

2. LOCALIZATION

In this section, we describe the basic localization framework that we use and present experimental results for its deployment in an office building. Similar to our previous work [31], our current system uses Markov localization [49]. However, rather than measuring every base station’s signal intensity distribution at points spaced 1.5 meters apart, we instead collected signal intensity measurements for whole offices and hallway segments, treating the entire office or hallway segment as a single position. The average area of each such position was 24.6 square meters (265.1 square feet). Hallways and large rooms (such as lecture halls) were broken up and treated as multiple positions, each about the size of a large office. The distribution of signal intensities for each base station was then fit to a normal distribution. We experimentally evaluated this distribution-fitting approach against the histogram approach used in our previous work, and our results show that it provides a substantial increase in robustness and a decrease in the number of observations required to train the sensor model. These improvements are in addition to the improvements gained by switching to a topological map from a geometric map.

2.1 802.11 wireless networking

Our localization system is based on the 802.11 wireless networking protocol, which is inexpensive and widely deployed on college campuses and in commercial offices. Likewise, most new laptop computers and PDAs have built-in support. 802.11 uses 11 channels in the 2.4 GHz industrial, scientific, and medical (ISM) band. Signal propagation in this band is complex, as many previous studies have confirmed [31, 46, 48].

As a part of its normal operation, client-side wireless hardware measures signal intensity from base stations to determine the best base station with which to associate. As a result, this mechanism is a part of the 802.11 specification, and the functionality is readily available in the hardware device driver. The 802.11 network card tunes into each channel in turn, sends a *ProbeRequest* packet and logs any corresponding *ProbeResponse* packets it receives [26]. Doing this for all 11 channels takes approximately 1.6 seconds with the combination of hardware and drivers we used, as described in Section 2.3.1. Our localization system uses the signal intensities observed from this process.

2.2 Localization models

2.2.1 Bayesian localization framework

The basic *localization problem* consists of determining an agent's *state* (or position), s^* , given one or more *observations*. The problem can be modeled by using a finite state space $S = \{s_1, \dots, s_n\}$ and a finite observation space $O = \{o_1, \dots, o_m\}$. Each state s_i corresponds to the case of the agent being in cell i .

In a probabilistic localization framework, the agent's estimate of its state is represented as a probability distribution $\bar{\pi}$ over S , where $\bar{\pi}_i = P(s_i = s^*)$. This method is useful since it can quantify the uncertain relationship between state and observation. In the Markov localization (ML) approach [49], the probability distribution over the observation space is determined completely by the current state. In particular, the relationship between state and observation can be represented by a matrix of conditional probabilities which encode the probability of observing $o_j \in O$ given that the agent is in state s_i , which is written $P(o_j|s_i)$. This matrix of conditional probabilities is referred to as the *sensor model*. Suppose the agent has a prior estimate π of its state and observes o_j . An updated estimate π' is computed using Bayes' Rule as follows:

$$\bar{\pi}'_i = \frac{P(o_j|s_i) \bar{\pi}_i}{\eta},$$

where

$$\eta = \sum_{i=1}^n P(o_j|s_i) \bar{\pi}_i.$$

The quantity η is the normalizer for the estimate and is sometimes referred to as the *confidence*. The confidence value can be used to quantify how certain the new position estimate is. In particular, the confidence value can be used for several different algorithmic extensions to Markov localization. By examining confidence, the localizer can choose between several different strategies in the case where one strategy is failing systematically. Important examples include the sensor resetting localizer [32] and various hybrid Monte Carlo localizers [53]. The confidence is also used to calibrate the system, as described in Section 4.

2.2.2 Gaussian fit sensor model

In our implementation, we fix a set $B = \{b_1, \dots, b_k\}$ of base stations and a set $V = \{0, \dots, 255\}$ of signal intensity values. The

observation set consists of $O = B \times V$. In this paper, we model the signal intensity as a normal distribution determined by the state and base station. Given state s_i and base station b_j , the signal intensity distribution is determined by its mean $\mu_{i,j}$ and standard deviation $\sigma_{i,j}$. The probability of observing $(b_j, v) \in O$ at state s_i is given by

$$P((b_j, v)|s_i) = \frac{G_{i,j}(v) + \beta}{N_{i,j}},$$

where

$$G_{i,j}(v) = \int_{v-1/2}^{v+1/2} \frac{e^{-(x-\mu_{i,j})/(2\sigma_{i,j}^2)}}{\sigma_{i,j}\sqrt{2\pi}} dx.$$

$G_{i,j}(v)$ is a discretization of a Gaussian probability distribution with mean $\mu_{i,j}$ and standard deviation $\sigma_{i,j}$. $P((b_j, v)|s_i)$ adds a null hypothesis and normalizes the resulting distribution. β is small constant used to represent the probability of observing an artifact and $N_{i,j}$ is a normalizer such that

$$\sum_{v=0}^{255} P((b_j, v)|s_i) = 1.$$

2.2.3 Histogram sensor model

Our previous work on localization with 802.11 represented the sensor model explicitly [31]. In this explicit model, each $P(o_j|s_i)$ is stored in a table. We call this method the *histogram* method since for each s_i , the $P(o_j|s_i)$ are determined by the normalized signal intensity histograms recorded during the training phase.

The histogram model can accurately represent non-Gaussian signal intensity distributions which can only be grossly summarized by a best-fit Gaussian curve. However, as we will see in Section 2.4.1, this does not necessarily give increased localization accuracy; the training can capture transient minor modes, or miss minor modes entirely. Also, the Gaussian model can be described by only two parameters for each base station and cell; keeping the entire histogram requires as much as 30 times more storage.

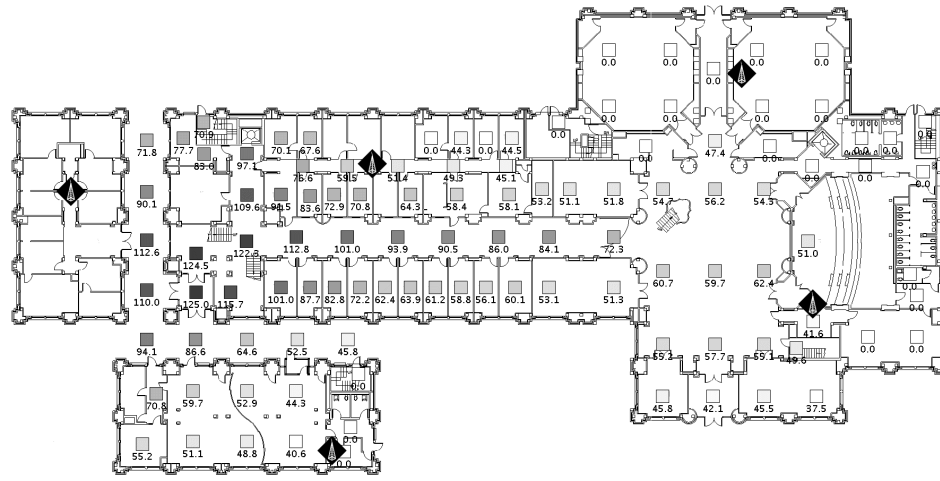
2.3 Experimental setup

2.3.1 Hardware overview

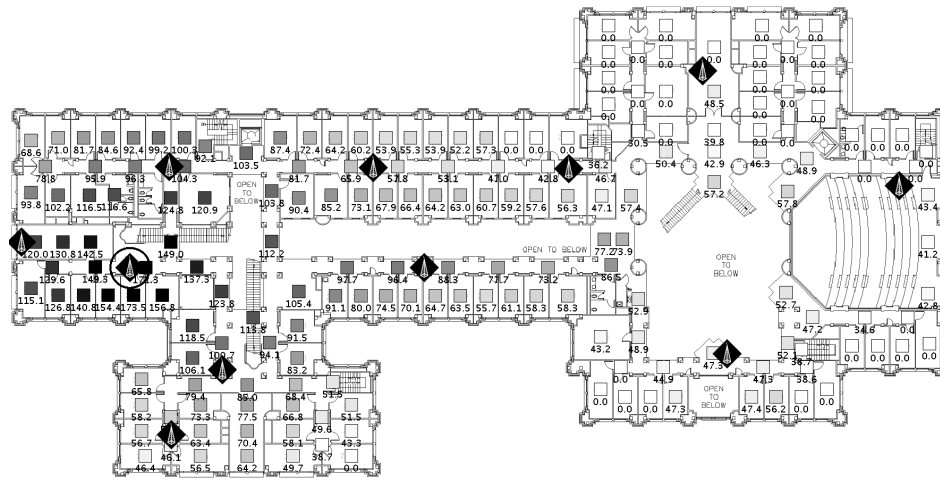
Our building has 27 Cisco Aironet 1200 Series base stations with 802.11a/b support, which were installed over a year ago; their locations were chosen so as to provide consistent coverage throughout the building. In addition to these, we used signals from six other base stations in adjacent buildings that covered at least part of our building; thus, our signal space has 33 dimensions. During both training and testing, we occasionally observed transient stations with ESSIDs like `Linksys` and `itcomputer`, which we ignored. The locations of these base stations remained fixed for all of our experiments.

On the client side, we used D-Link AirPlus DWL-650+ WLAN PCMCIA cards with the Texas Instruments ACX100 chipset. Our experiments were performed on a Dell Latitude X200 laptop running the Linux 2.4.25 kernel and an IBM Thinkpad T40p running the Linux 2.4.20 kernel. We used the open-source ACX100 driver from SourceForge [3] with a few modifications for stability. We also optimized the code that handles base station scanning to reduce the time required for each individual scan.

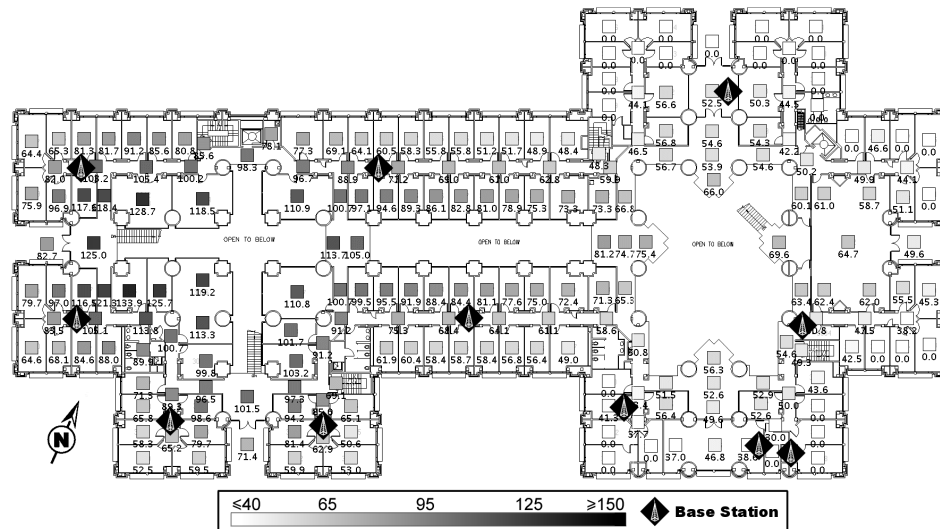
Base station scans were performed on-demand using a standard function in the Linux Wireless API; the network card does not need to be in a special mode to initiate such a scan. As discussed in Section 2.1, base station scanning is a standard capability of 802.11 wireless network cards. However, while the wireless network card is performing a scan, it cannot be used for data traffic.



(a)

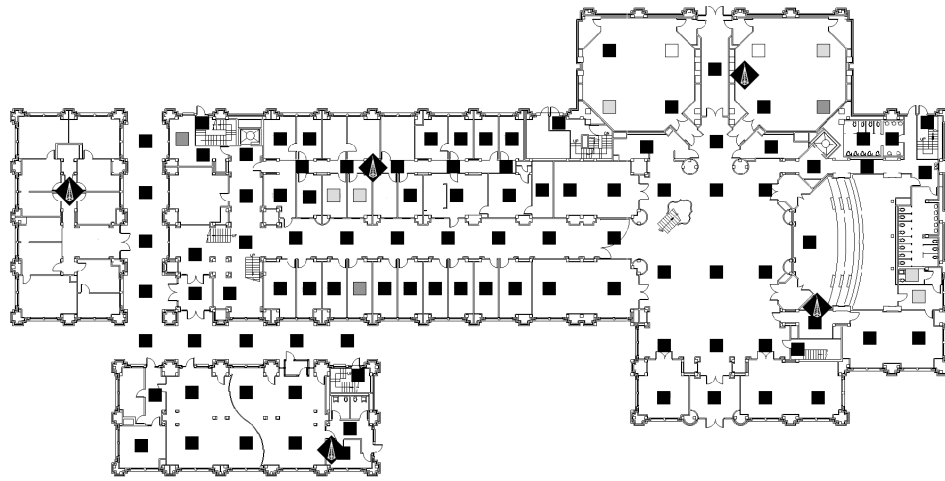


(b)

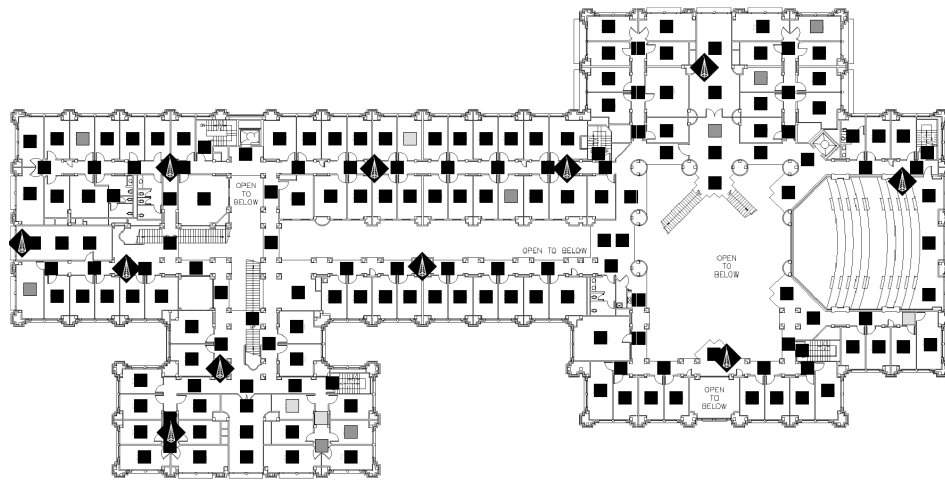


(c)

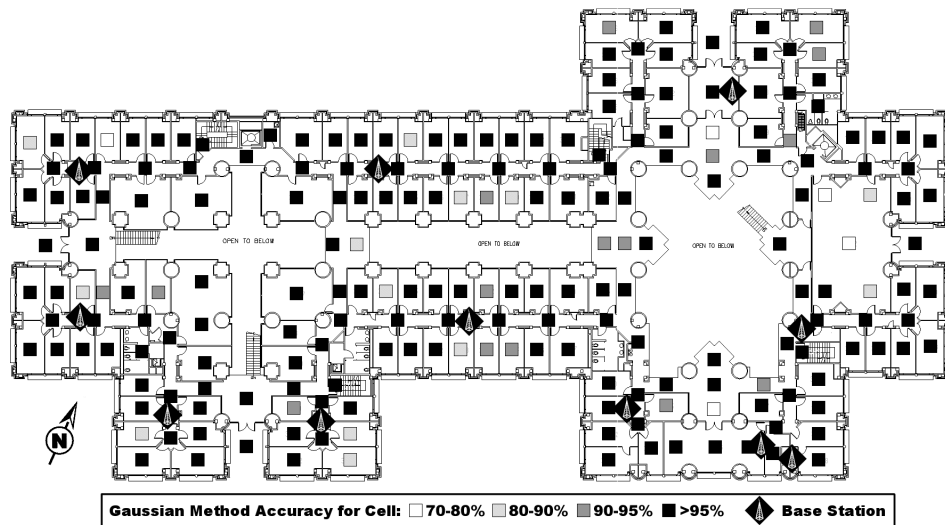
Figure 1: Sensor map within Duncan Hall for a base station located on the second floor. Base stations are represented as black diamonds with white antennas; the base station from which this sensor map was generated is circled. (a) is the first floor; (b) is the second floor; (c) is the third floor. Each shaded square represents a single training and testing cell. Darker squares indicate stronger readings.



(a)



(b)



(c)

Figure 2: Map showing robustness of the Gaussian localization algorithm in Duncan Hall. (a) is the first floor; (b) is the second floor; (c) is the third floor. Each shaded square represents a single training and testing cell. The darkness of the square indicates the percent of trials for which the localizer indicated the correct location at that position.

2.3.2 Our building

We deployed our location-sensing system in Duncan Hall on the Rice University campus, a building which consists of three stories plus attic and basement utility spaces. Duncan Hall has over 200 offices, as well as several conference rooms, five classrooms, and an auditorium. The total area of the building is 12,558.4 square meters (135,178 square feet). Maps of the three floors of Duncan Hall are shown in Figures 1 and 2.

The most notable feature of our building is its complex geometry. The building has a large clerestory ceiling; the main hall on the east side of the building, the wide hallway connected to it, and staircases beginning at the hall and hallway are all open above. The hallways surrounding the atrium and the hallways passing over the wide hallway on the second and third floors all contain balconies overlooking the first floor, and many of these are open to the clerestory ceiling above. In addition, all of the interior offices on the third floor are open above, and all but eleven of the interior offices have windows into the interior of the building.

2.3.3 Topology

We divided the building into 510 different cells on the topological map. This was done manually by placing cells on a floor plan of the building and took approximately one hour; for larger buildings, however, this process can be easily automated. Typically there is one cell per office. For large labs and lecture halls, however, the standard deviation of reported signal intensities would have been too high for localization to be usable. As a result, we assigned different cells to different regions of these rooms; these different cells were trained separately, but could be treated as a single cell for the purpose of localization. We also assigned cells to hallway segments. Figures 1 and 2 show how these training points are distributed throughout the building.

Cell sizes varied over the building. The typical office size (and therefore, cell size) is approximately 2.7 by 4.9 meters (9 by 16 feet). The largest room trained as a single cell is approximately 6 by 6 meters (19.7 by 19.7 feet). Most hallways are 1.6 meters (5.3 feet) wide, and are partitioned into cells of segments approximately 5.7 meters (18.7 feet) long. We also trained cells for outdoor locations, including third-floor balconies and a first-floor arcade.

To track agents as they move, we built a transition graph over the set of cells. This graph contains 1,159 edges (including self-transition edges), and the average out-degree is 3.55. It represents navigable paths in our building, encoding the fact that one cannot pass through walls except via doors, and one cannot switch floors except via a staircase.

2.3.4 Training

We obtained a master key for the entire building and collected at least 100 base station scans in each of the 510 cells. The person doing the training spent approximately 2.7 minutes in each cell. This person walked around slowly in order to cover the entire cell. The main goal in collecting the training data was to get a signal sample for each part of the cell; we did not concern ourselves with the relative position of the operator performing the training. Data collection took 28 man-hours overall; however, we collected many more scans than we needed to ensure that we would have independent data to experiment with. Had we only collected one minute of training data per office, the minimum we recommend for production use, training could have been accomplished in less than half the time. Keep in mind that data collection can be done concurrently; we collected our data using two operators, doubling our throughput.

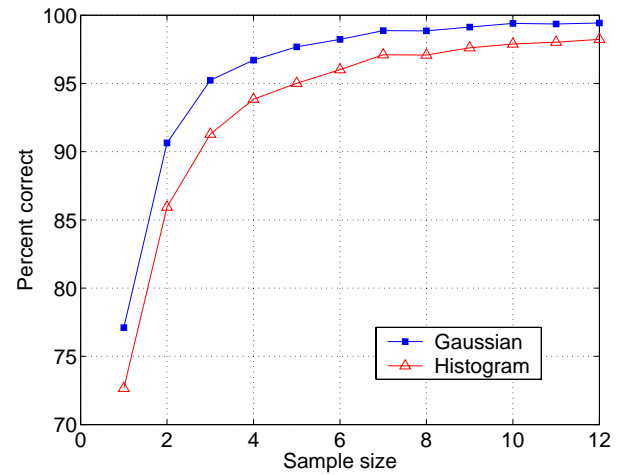


Figure 3: Bulk accuracy of localization methods after different numbers of observations.

We collected a total of 51,249 scans. On average, each scan contains a signal intensity reading from 14.86 of the 33 base stations. We observed intensity values ranging from 1 to 217; thus, we estimate about 7.5 bits of usable information. When examining the intensity histograms, we found three fundamental types. Most of them were very close to Gaussian, so the Gaussian fit worked very well. Some were sparse, indicating that the base stations were almost out of range; in these cases, the Gaussian fits had fairly large standard deviations. A few were bimodal; the estimated mean was in the middle, with a large standard deviation. Initially, we experimented with a bimodal weighted Gaussian fit, but our results for the single-mode estimator show that the improvements in accuracy would be marginal.

The sensor map of the entire building for a second-floor base station is shown in Figure 1; the base station in question is circled. As expected, signal intensity degrades fairly consistently as distance increases from the base station. There are several interesting phenomena of note. First of all, we can still reliably get a signal from the base station while outside or in a disconnected part of the building (that is, through two exterior walls and windows). Second, the base station can be detected from across the building even on different floors. Finally, at long distances, some offices will see the base station while neighboring offices see nothing. This could be caused by multipath effects or by other variations in building geometry that result in favorable signal propagation.

2.4 Experimental results

2.4.1 Localization accuracy

The goal of this experiment was to determine the basic localization performance of our system using Gaussian-fit curves and to compare it with a system using the same training data but retaining the full histogram of signal intensity observations. We chose five scans at random for each of the 510 cells and removed them from the training set. The remaining scans were used to train our localizer. Then, for each cell, we used the scans we had removed from the training set as input to the localizer and attempted to locate ourselves. We performed this experiment 100 times, removing different scans each time.

Figure 2 shows the test cells on the map of our building and the percentage of experimental trials in which the Gaussian method

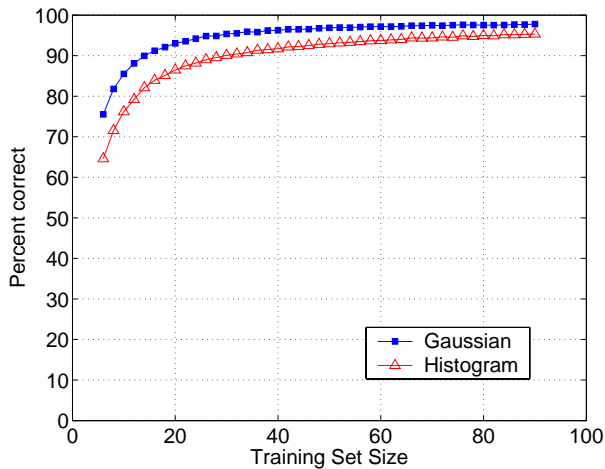


Figure 4: Training set size versus accuracy for the Gaussian and histogram methods.

returned the correct cell after five scans. In all cases, the Gaussian method determined the correct cell in at least 70% of trials; at all but a few locations, the localizer returned the correct cell in more than 90% of experimental trials. While the histogram method was likewise correct in at least 90% of trials at most locations, there were several cells where the histogram method was correct in fewer than 50% of trials. Over all experimental trials, the Gaussian method was correct in over 97% of trials. The histogram method was correct in over 95% of trials. While the histogram method’s overall accuracy was comparable to the Gaussian method’s accuracy, the Gaussian method has better behavior in pathological cases, typically returning a cell that is off-by-one from the correct location. This result is discussed in more detail in Section 3.1 and illustrated in Figure 8.

We wanted to explore the behavior of our system as we varied the number of observations from which the system infers location. The fewer observations required to infer a device’s location, the faster this inference can be generated; each additional observation adds an approximately 1.6 second delay in generating each location estimate. We ran the same experiment as above, but chose from one to fifteen random scans for each cell to use for testing the localization. We performed this experiment 100 times for each cell. The results for one through twelve scans are shown in Figure 3; after twelve scans, the graphs show almost no further variance.

The results show that using one scan, both methods successfully infer the location in over 70% of cases. 90% accuracy is achieved with at least two scans for the Gaussian method, and with at least three scans for the histogram method. It takes approximately 1.6 seconds to perform a scan, so at that accuracy, we can localize the agent once every 3.2 seconds using the Gaussian method, and once every 4.8 seconds using the histogram method. Note that different hardware and driver combinations might be able to perform a scan faster, leading to shorter latencies between usable localization results.

2.4.2 Training set size

To evaluate the behavior of our localization system with smaller training sets, we chose training set sizes ranging from six to 90 samples per cell. When it takes 1.6 seconds to collect each sample, any reduction in the necessary training set size per cell will add up to a significant reduction in data collection labor over a large

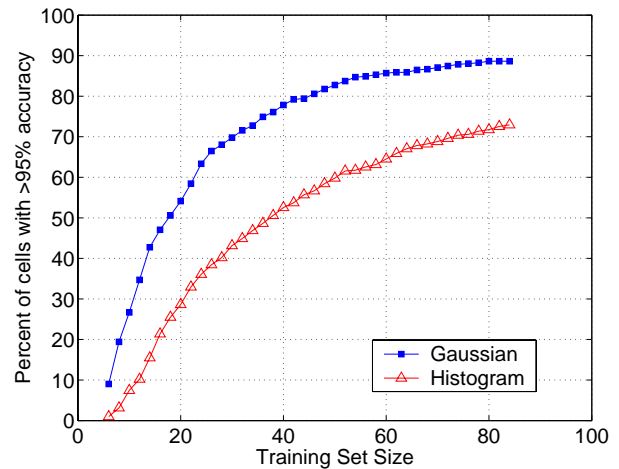


Figure 5: Training set size versus percent of cells where 95% of trials returned the correct location.

building. As before, we chose five scans at random from our data to be our experimental scans. We then pruned the training set to the appropriate size by removing training points at random and finally attempted to localize to each cell. We performed this test 100 times. The percentage of correct location estimates over all experimental trials for the Gaussian method versus the histogram method is shown in Figure 4.

The graph shows that both methods have good overall accuracy even at low training set sizes. However, the histogram method tends to require close to twice as large of a training set as the Gaussian method to attain a similar accuracy. The Gaussian method attains a 90% accuracy using only 16 training points; the histogram method requires 30 training points to attain this accuracy. Similarly, the histogram method requires 84 training points to attain a 95% accuracy; the Gaussian method requires only 30 training points, corresponding to only 48 seconds in each office.

Accuracy also varies by location. Figure 5 graphs the percentage of cells where at least 95% of experimental trials generated a location estimate corresponding to the actual location. This graph shows that the Gaussian method requires 24 elements in its training set to attain a 95% accuracy over 60% of the cells, 32 elements in its training set to attain a 95% accuracy over 70% of the cells, and 46 elements for a 95% accuracy of 80% of the cells. By contrast, the histogram method needs 52 elements to attain this accuracy over 60% of cells, and 74 elements in its training set to attain this accuracy over 70% of cells. We did not train with enough points for histogram to get 95% accuracy at 80% of cells. For other cut-off percentages (that is, other than 95%), we again observed that approximately half the number of training points are required to attain comparable levels of accuracy for the Gaussian method versus the histogram method.

Finally, we compared how many training points are required at individual cells before the localizer generates a correct location estimate in at least 95% of experimental trials. Table 1 shows the number of cells for which an accuracy of 95% can be achieved with the histogram method and the Gaussian method as the number of training points increases; the caption provides detailed information on how to interpret the numbers in the table. At only two cells does the Gaussian method require more training data than the histogram method to attain a 95% accuracy. At over $\frac{3}{4}$ of the points, the Gaussian method requires less than 30 training points. By contrast,

Method # of Training Points	Histogram < 30	Histogram 30 – 60	Histogram > 60
Gaussian < 30	234	105	46
Gaussian 30 – 60	2	17	68
Gaussian > 60	0	0	67

Table 1: Table showing number of cells at which the histogram and Gaussian methods first correctly localize to the cell in 95% of experimental trials as the training set size increases. The rows and columns are labeled with the number of scan records in the training set for each method we used. For instance, the 46 in the top right corner indicates that for 46 cells, the Gaussian method requires fewer than 30 training points to achieve 95% accuracy, and the histogram method requires over 60 training points to achieve this accuracy.

for most of the points, the histogram method requires at least 30 training points for 95% accuracy, and for over $\frac{1}{3}$ of the points, it requires over 60 training points. For most points, therefore, a 60-second training phase at each point (corresponding to a 37-element training set) is sufficient to localize most points to very good accuracy using the Gaussian method.

2.4.3 Base station density

Localization accuracy is also influenced by the number N of base stations in the building. If N is reduced, less information is available to the localizer, and thus the accuracy decreases. To quantify this effect, we performed another experiment in which we varied N by randomly removing some of the 33 base stations from our data set. In doing so, we ensured that at least one base station was still visible from each cell, and that at least 50 nonzero scans per cell remained. From the resulting data set, we took five random scans per cell and ran them through a localizer that was trained with the remaining scans.

The experiment was performed with both the Gaussian method and the Histogram method. For each value of N , we chose 20 random subsets of base stations and performed five trials for each subset. We report the overall fraction of trials in which the localizer was able to determine the correct cell, as well as the 20th and 80th percentiles.

Figure 6 shows our results. Even with only 17 instead of 33 base stations, the Gaussian method can determine the correct cell in over 90% of the trials. For lower values of N , the accuracy declines rapidly, while the fluctuations are significantly higher. This is because at lower densities, the exact placement of the base stations starts to matter; also, the number of scans available to the localizer decreases because some of them contain only values for base stations that have been removed. If this were compensated by using an even larger data set, the results for lower densities would improve. However, in real-world wireless network deployments, it is reasonable to expect some redundancy of base station coverage to improve the quality and robustness of service.

3. TIME-VARYING PHENOMENA

The localizer we have presented in the previous section assumes a static environment and a stationary agent. Neither assumption is realistic. The observed signal intensity distributions will often differ from the distributions estimated in the training phase due

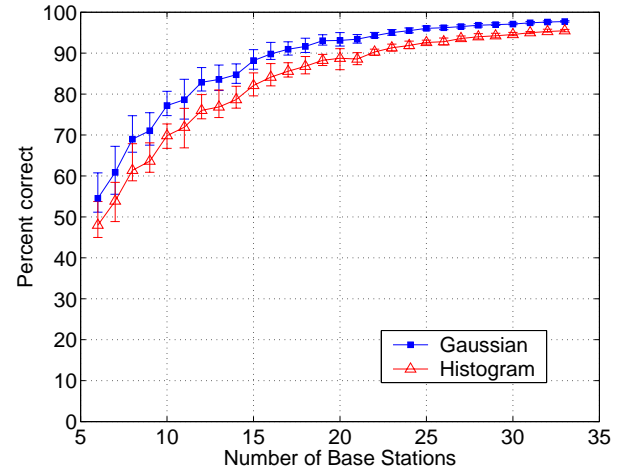


Figure 6: Impact of base station density on localization accuracy.

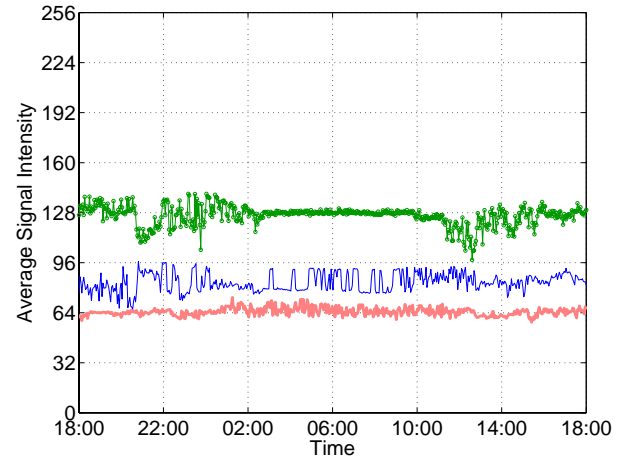


Figure 7: Signal intensity variation over a 24-hour period for three base stations measured from a laptop in a fixed location.

to a myriad of time-correlated phenomena. These phenomena include environmental properties such as attenuation due to people in the building or building residents opening and closing their office doors. Likewise, transient interference can be caused by other electronic devices including microwave ovens, Bluetooth devices, and cordless phones. Furthermore, a 2.4 GHz frequency corresponds to a 12.5cm wavelength, implying that multipath fading effects may be experienced even with small changes in the operator’s location. These dynamic environmental influences can cause the observed signal intensity to vary over both small and large timescales. The movement of the operator in the environment further complicates the task of maintaining an accurate position estimate.

3.1 Signal variations due to office traffic

Over the course of the day and throughout the night, many changes occur in the environment which affect the observed signal intensity. Each of these changes tend to be local and transient but since the nature and frequency of these events varies with the time of day, we expect that, on average, the signal intensity distribution changes globally on a larger timescale. In order to estimate the size of this

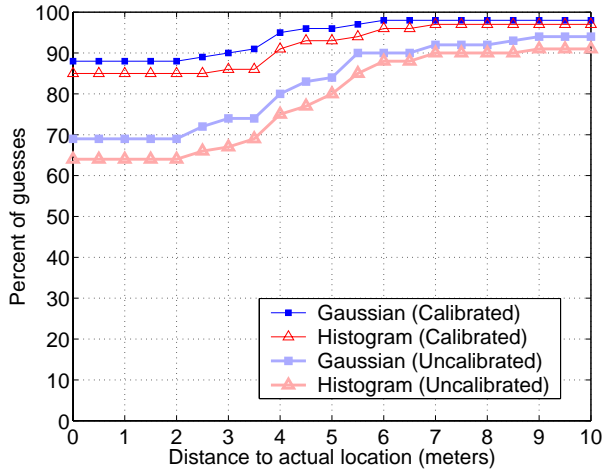


Figure 8: Basic daytime performance for 27 cells. The results marked “calibrated” were obtained using the calibration technique from Section 4.2.

effect, we collected scans at a fixed location (an office) over a 24-hour period. The resulting 52,900 scans were divided into groups of 100, and the signal intensities were averaged over each group. Figure 7 shows the result for three different base stations. There are noticeable variations during the day. At nighttime, some of them become less pronounced or more regular, while others disappear almost entirely.

Time-varying effects have severe implications on the accuracy of localization. To quantify these, we performed localization experiments in 27 different cells at around 11:00 AM, when there is relatively heavy traffic in the building, including students either in class or going to or from class. We collected approximately 30 scans in each cell and then ran each possible subset of five consecutive scans through the localizer; the probability vector was initialized with a uniform distribution each time. The results are presented in Figure 8. We observed mediocre results; using the Gaussian method, less than 70% of location estimates were correct, with the bulk of observed errors within 5.5 meters of the correct location. These results and techniques to improve them are discussed further in Section 4.

3.2 Tracking

Another time varying phenomenon we examined is the movement of the agent. Markov localization works well as a single-shot localization algorithm or for a stationary agent; however, for a moving agent, the prior position estimate will hamper correct localization. A simplistic solution can be obtained by resetting the distribution $\bar{\pi}$ to a uniform distribution over all states between each burst of observations. A more elegant and effective solution is to update the state estimate between each set of observations using a Markov chain that encodes assumptions about how the agent can move from state to state.

Suppose at time t , the state estimate is $\bar{\pi}^t$. Between time t and $t + 1$, the agent moves in some unknown way. At time $t + 1$, the observations o_1, \dots, o_k are received. The state estimate at time $t + 1$ is computed as follows:

$$\bar{\pi}_i^{t+1} = \frac{\prod_{j=1}^k P(o_j | s_i) \bar{\pi}_i^t}{\eta},$$

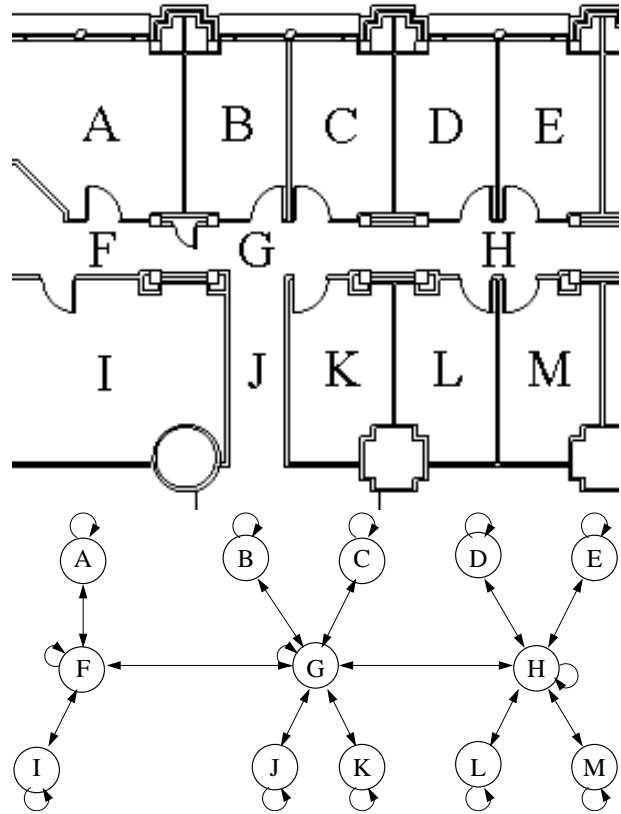


Figure 9: The floor plan for part of Duncan Hall and the corresponding Markov chain.

where

$$\bar{\pi}^{t+1} = A \bar{\pi}^t.$$

As before, η is a normalizer that ensures $\bar{\pi}^{t+1}$ is a probability vector. The probability matrix A encodes the Markov chain, which can be thought of as a finite state machine (Figure 9). States represent cells, and an edge from state s_i to state s_j indicates that cell j can be reached directly from cell i . Also, each edge is assigned a transition probability $A_{i,j}$. In our implementation, we gave a fixed probability to the self-edge at each state and distributed the remaining probability evenly across its outgoing edges.

3.3 Tracking experiments

We wanted to evaluate the effectiveness of Markov chains when tracking a moving agent. First, we randomly chose four way-points in our building. Then we simulated a person following the shortest path between these way-points; the simulated agent remained at each way-point between 10 and 15 seconds, and moved with a constant speed between 0 and 4.5 meters per second (between 0 and 10.1 miles per hour) from one way-point to the next. Every 1.6 seconds, we chose a random scan from the closest cell to the agent’s simulated location.

This timing simulates the agent performing back-to-back base station scans. The agent would not be able to communicate over the network while tracking. As a compromise, the agent could interleave scans and communication, e.g. by using the interface for data traffic for 1.6 seconds in between each 1.6-second scan. In

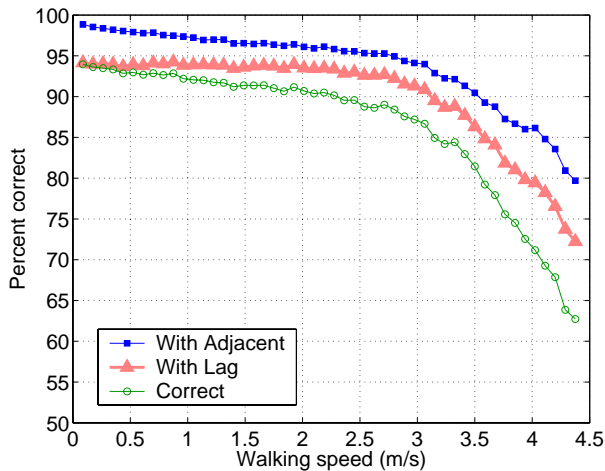


Figure 10: Accuracy of dynamic tracking as a simulated person walks around our test area. *Correct* is the overall percent of correct location estimates. *Lag* is the overall percent of location estimates that match either the current or the previous cell. *With Adjacent* is the overall percent of location estimates within one location cell in our topological model.

this experiment, a person using such a system would appear to be moving at twice her actual speed.

These scans were then run, in order, through the localizer. We also passed the location estimate through a hidden Markov model of the agent’s movement through the environment. The initial probabilities for the hidden Markov model were set to 1.0 for the correct cell and to 0.0 for all other cells. We performed this experiment 250 times for each speed. The results are shown in Figure 10.

The *Correct* result is the overall percent of correct location estimates. This value decreases slowly until a velocity of 4 meters per second (8.9 mph), and even at this speed, the localizer has an accuracy of 71%. The *Lag* result is the overall percent of location estimates that match either the current or the previous cell. By this metric, our method experienced a similar drop-off of accuracy at 4 m/s. The localizer had an accuracy of over 79% at this speed. Finally, the *With Adjacent* result is the overall percent of location estimates within one location cell in our topological model; by this metric, the localizer had an accuracy of 86% at 4 m/s.

This demonstrates that our localization method, when coupled with a hidden Markov model of motion, can accurately track even a fast-moving target. As expected, the overall accuracy is lower than for static localization. Even at a slow walking pace, only four scans might be registered before the agent enters a new cell, so it is unsurprising that localization accuracy is lower for moving than for stationary agents. The hidden Markov model helps the system by, in effect, anticipating this movement and rejecting unlikely measurements when they would otherwise predict impossible transitions. Also note that different hardware and driver combinations might be able to complete a scan faster than the 1.6 seconds we experienced; this would greatly improve our results.

Another interesting phenomenon we were concerned about was that the tracker might get “stuck” in an office adjacent to the agent’s current location. Because there were no direct edges connecting adjoining offices, the tracker might not make the transition. Although we considered adding “phantom” edges to the transition matrix A to account for this behavior, the tracker would, in practice, follow

first the edge from the adjacent office to the hallway, and from there to the correct office, thus correcting for such errors automatically.

3.4 Miscellaneous effects

To illustrate the impact of time-varying phenomena on tracking performance, we report some insights from our practical experience with the system. One of the authors was using the tracker over a normal office day, during which he attended a lecture and a presentation, worked at his desk, and walked from office to office. The overall performance was very satisfactory; the estimated location occasionally jumped to an adjacent cell, but generally matched the true location well.

The presentation, which was held in a conference room full of students, turned out to be a worst-case scenario. The signal was not only heavily attenuated, but also changed over time, for example when a fellow student leaned over and thus moved closer to the antenna. This caused the estimated location to jump between the three different cells in the conference room, and occasionally to the cell right outside the door. Similar effects were observed when the author met other students in the hallways and was asked to explain the experiment. As soon as the other person moved close to the antenna in order to watch the location estimate, the estimate jumped to an adjacent office.

4. CALIBRATION

The sensor maps built by our method can only be guaranteed to work for localization if they are used in the same environment as during the training period. However, as shown in the previous section, the environment can change significantly over the course of the day. Moreover, the signal intensity values reported by the hardware depend on various factors, including the chipset and the antenna, and can vary considerably between different 802.11 implementations. Therefore, a method is needed to adapt the sensor map to the environment in which it is to be used.

Fortunately, we observed that the effect of environmental changes, including both time-varying effects and different hardware, can be closely approximated by a linear relationship. Thus, the sensor map can be adapted to a new environment simply by learning two parameters. This process, which we refer to as *calibration*, should require little or no user intervention; ideally, it would be performed in the background, thus enabling the localizer to work “out of the box.”

In this section, we first describe the model we use for calibration and give several examples of different configurations and the corresponding parameters. Then we present three different calibration methods, spanning the range from completely manual to completely autonomous.

4.1 Model

The calibration problem can be formulated as follows: Given a sensor map and an 802.11 device in a certain environment, find a *calibration function* c that maps an observed signal intensity value i to the value $c(i)$ that would have been reported by the device that was used to generate the sensor map. If c is known, $c(i)$ can be given as an input to the localizer, and the original sensor map can be used unmodified.

As Tao et al. [48] first observed, there is a linear relation between transmission power level and received signal strength as reported by 802.11 hardware. In our experiments, we discovered that the effects of hardware variation and some time-varying phenomena appear to be linear as well. That is, the calibration function can be

Chipset	Relation
ACX100	$c(i) = i$
Prism	$c(i) = 0.85 \cdot i - 43.5$
Atheros	$c(i) = 2.77 \cdot i - 409.5$

Table 2: Linear relationships between several different 802.11 cards and the ACX100 card we used in training. i is the value reported by the hardware, and $c(i)$ is the equivalent value that would be reported by the ACX100, and that can be input into the localization system to accurately determine the device’s location.

closely approximated by the linear relationship

$$c(i) = c_1 \cdot i - c_2.$$

Thus, it is sufficient to learn the parameters c_1 and c_2 in order to adapt a given sensor map to a new environment. This can be accomplished in various ways; for example, one can collect some measurements at well-known locations and compute the least-squares fit between the observed values and the corresponding values from the sensor map.

Using this method, we found the parameters for a number of different cards. These are listed in Table 2. The ACX100 is the card we used for training, so its calibration function is the identity function. *Prism* is a Linksys WPC11 PCMCIA card based on the Intersil Prism2 chipset. *Atheros* is a Mini PCI card with an Atheros chipset and using the IBM Thinkpad T40p’s built-in antenna.

Figure 11 shows the effects of calibration for the Atheros chipset. This ‘unadjusted’ graph was generated using pairs (i_R, i_M) of intensity values, where i_R is the reference value from the sensor map for a certain cell and base station, and i_M is the corresponding value measured with the Atheros card. The ‘adjusted’ graph shows $(i_R, c(i_M))$, clearly indicating that after calibration, the two values are almost identical.

Note that the signal intensities reported by the Atheros chipset were 8-bit values as in the ACX100 case, but we observed only values between 163 and 224, so there are only 5.9 bits of usable information.

That is not to say that the difference in signal strength reporting between any two cards is always a linear relation. In particular, different cards may use different techniques to actually measure the signal strength. As Steger et al. [47] demonstrated, different cards behave differently in the face of varying signal conditions. In addition, as indicated by our results, the mapping from the actual signal strength to the number returned by the hardware is arbitrary, will vary from one chipset to another, and need not be linear. However, in all the cards we tested, the signal strength readings were linear relations of one another.

4.2 Manual calibration

As mentioned earlier, the parameters of the calibration function can be found by computing a linear fit for a set of measured signal intensities and the corresponding values from the sensor map, e.g. by applying the least-squares method. First, we must collect enough value pairs to perform this calculation. In our prototype implementation, this is done by moving the device to several different cells. In each cell, the user presses the ‘calibrate’ button, prompting the device to collect a few scans, and then indicates the current cell on a floor plan of the building. Since in Duncan Hall, each cell contributes value pairs for 14.86 base stations on average, a small number of cells (three to five) was usually sufficient.

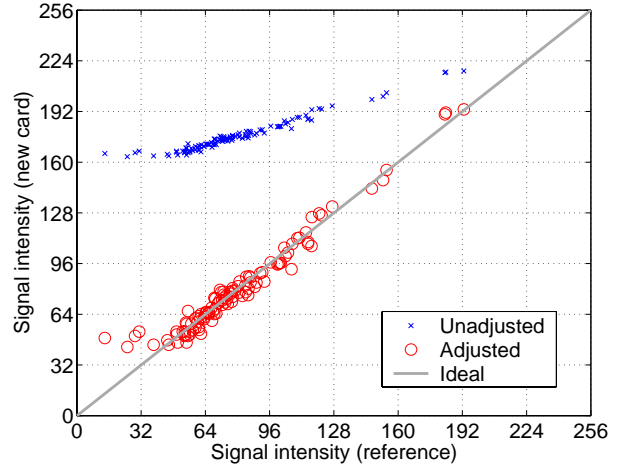


Figure 11: Effect of calibration on the signal strength values reported by the Atheros chipset. The intensity values shown are averages over at least five samples.

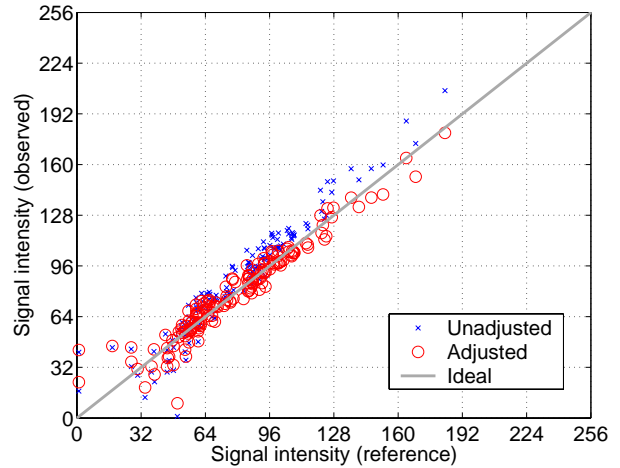


Figure 12: Average signal intensity values, before and after recalibration for time-varying effects.

Figure 12 shows an example result from such a calibration. In this case, the 802.11 hardware was the same as during the training period, but the measurements were taken at daytime during heavy office traffic. Clearly, both the constant offset and the linear factor changed. Yet, after calibration, the signal intensity values correspond almost exactly to the ones from the training phase.

In order to quantify the effect of calibration for time-varying effects, we ran the localization with and without performing calibration. The result is shown in Figure 8. Without calibration, the results are mediocre: less than 70% of location estimates are correct, and 90% of estimates are within 5.5 meters for the Gaussian method. After calibration, results are greatly improved: 88% of location estimates are correct, and 90% are within 3 meters. This experiment suggests an important conclusion: that a single linear-fit captures most of the deviation induced by slow timescale phenomena. In other words, the signal intensity shifts due to slow time-varying effects seem to be homogeneous on average across various locations. Qualitatively, we have observed that running localization without tracking, during the day, is a bit noisy, lags a

bit, and is prone to localizing into the room adjacent to the user. Once we run the calibration in three or four cells, the localization is extremely stable and very rarely makes mistakes.

4.3 Quasi-automatic calibration

Manual calibration is clearly effective, but has the disadvantage of requiring the user to specify the current cell. Surprisingly, however, calibration can be performed without this information and using *only* a set of scans from several different – but unknown – cells.

Our second calibration method takes advantage of the fact that the observation space is both sparse and non-linear, so there is almost never a linear mapping between observations from different cells. Hence, when an incorrect calibration function is used, the calibrated intensity values do not match any reference values from the sensor map, and the confidence value η produced by Markov localization (see Section 2.2.1) is low for all cells; it is high only if *both* the calibration function and the cell are correct. Therefore, the parameters c_1 and c_2 can be learned by attempting Markov localization and by choosing values such that the confidence η is maximized.

4.4 Automatic calibration

Although the quasi-automatic method involves less user interaction than the manual method, it still requires the user to press a ‘calibrate’ button from time to time. However, in order to obtain optimum performance, the user will have to recalibrate several times over the course of the day, which is cumbersome and, in the case of manual calibration, requires a certain familiarity with the building. It would be clearly preferable to have an entirely hands-off solution.

Toward this end, we have been investigating the problem of running localization, tracking, and calibration simultaneously. Our initial results are promising but do not yet match the results we have seen with supervised calibration for online localization and tracking. The basic technique we have been considering uses a history of recent observations as a training sample to construct an estimate of the calibration parameters that are then used to process future data. This algorithm runs in parallel with the localization process. We use an expectation-maximization algorithm (E-M) [52] that computes a fixed-point, iterating between inferring a sequence of location estimates from the history and then choosing c_1, c_2 to maximize the probability of these estimates occurring. The observations and estimates are stored in a sliding window of between 10 and 45 seconds.

Our current implementation of simultaneous localization and calibration seems about as good as supervised calibration for static localization problems. In the tracking implementation, we have observed that the tracker is a bit sluggish and prone to place the user in adjacent rooms. Also, it seems to occasionally get stuck with a bad hypothesis that stays until the sliding window fills with new data. If the size of the sliding window is decreased then the tracker lags.

Another possible approach that we believe may be attractive is a Monte Carlo (particle filter) approach [18, 53] that maintains a set of c_1, c_2 hypotheses and gathers data to determine which hypothesis should be used. Where our current approach only maintains one hypothesis at a time, this approach would simultaneously try a large number of hypotheses, preventing the system from getting stuck with a local maximum and thereby missing globally optimal settings. In this framework, the confidence values from the localizer (η) could be used to discriminate between two hypotheses. Our

experiments and data analysis suggest that solving the problem of making a simultaneous localizer and calibrator is tractable.

5. DISCUSSION

5.1 Why a Gaussian fit?

Our most striking departure from previous work is that the most successful systems in the literature have used the entire signal intensity histogram. On the other hand, we have chosen to fit the sensor map data to Gaussian distributions. We chose this course for several reasons.

First, fitting the data to a Gaussian only requires storing two numbers for each base station and cell. Keeping the entire histogram requires at least 30 times as much storage. This reduction increases the speed and reduces the memory requirements for localization, making it more suitable for low-power embedded devices that may not have the resources of a modern laptop computer.

Furthermore, fitting to a Gaussian also provides some robustness benefits to our system. The Gaussian method tends to provide roughly the same accuracy of localizations for half the training effort (see Section 2.4.2). One reason for this is that if the entire histogram is used, the training might capture minor modes that are a result of time varying phenomena and might miss other minor modes not present in the training set. These minor modes will be covered by the normal distribution curve to which the data is fit in the Gaussian method. Also, previous histogram-based systems required taking as many as 500 scans to train each point. This would make it impractical to build a sensor map as large as the one we built without a significantly longer training time.

5.2 Choosing a training set size

Although most of our localization results are based on training sets with 90 elements, we determined that for our building, taking a 60-second training set (around 37 elements) was adequate for accurate localization in most of our building (see Section 2.4.2). The point of diminishing returns, in terms of accurately capturing the sensor map, seems to begin around 35 samples per point (see Figure 4). Of course this is a minimum; having additional training data can only help.

The optimal number of training points depends on a number of factors, including building geometry, base station density, and building usage. Although Duncan Hall has unusual geometry, the base station density is high; there are rarely fewer than five base stations in range, even in the corners of the building. Buildings with fewer base stations, lower base station density, or more opaque construction materials, would likely need larger training sets.

Buildings with interesting geometry, such as large open areas, tend to dilute differences in signal intensity, and require more training data. As the sensor map in Figure 1 shows, hallways tend to channel signals such that signal intensity drops at a regular rate going down a hallway. Large open areas tend to disperse signal, leading to much less distinction among cells.

To adequately measure signal maps in other buildings, experimentation may be necessary to determine the ideal set size. For our own building, we started by first collecting training data in a small region of the building. By observing the mean and standard deviations of this data, we could estimate how many samples were necessary for the system to converge. In our own case, we observed that, with 25 scans, the variation of the mean dropped below 2. For experimental purposes, we captured significantly more than 25 scans per cell to help verify our results.

It would be possible to encode the above technique into the training system. When the mean and standard deviation stabilize to

within a specified threshold, we can conclude that we have collected enough training data to accurately describe a cell. This check could be run in real-time.

5.3 Changes to the infrastructure

In this paper, we implicitly assumed that the sensor map accurately reflects the signal intensities throughout the building. However, this is only true as long as there are no fundamental changes in the environment, such as base station failures or major reconfigurations. While changes of this type are infrequent in practice, they may affect localization accuracy where they do occur.

If an individual base station fails, it does not respond to probe requests any more and thus changes the observations made from the surrounding cells. However, because our method only uses positive observations, i.e., probe responses actually received, the only effect this has on the localizer is that there is less information available, reducing accuracy and convergence speed. As long as enough other base stations are in range, the effect should be small (see Section 2.4.3).

Moving an existing base station requires the cells surrounding the old and the new position to be re-trained. However, since base stations are typically wall-mounted and require power and a network connection, they cannot be moved easily, so changes of this type should be very rare.

The appearance of transient base stations does not affect localization because the localizer can easily determine the set of acceptable stations from the signal map and ignore unknown stations. If a permanent station is added after the training phase, it can be used to improve accuracy by re-training the cells from which it is visible.

Some base stations choose their channels dynamically; thus, a major failure such as a power outage may cause the channel assignment to change. This actually happened once during our experiments, when a maintenance event required the entire building to be taken off-line. Although the base stations operated on different channels afterwards, we did not observe a significant change in accuracy.

5.4 Passive localization

Passive localization refers to localization in which the mobile device being localized is a passive participant in the localization process. While the device must be transmitting data to be tracked, it is not explicitly performing any part of the localization algorithm, and need not be aware that it is being tracked. Since signal propagation is a reversible operation, the same sensor map data should, after calibration, allow someone with access to enough receivers to track any transmitting device. While we've performed some experiments that tend to validate this, more experimentation is in order.

The most obvious application of passive localization is for locating an intruder on an 802.11 wireless network. Tao et al. [48] performed a study of this issue. Two problems they overcame were differences in hardware and differences in transmission power. Since both of these were fixed by mapping received signal intensity to the training set via a linear relation, the calibration technique we discuss in Section 4 should allow us to account for both of these variations. A promising avenue of future work is applying simultaneous localization and calibration (see Section 4.4) to automatically account for variations in hardware, movement, and transmission power manipulation on the part of the intruder.

Finally, more ambitious intruders might attack in coalitions, jointly transmitting packets using the same hardware address. This would make the attacker appear to be jumping all over the map. We

believe clustering algorithms may be able to adequately determine the number of attackers and separately localize each one.

There are of course privacy implications to being able to track any arbitrary device on an 802.11 network. Anyone who has physical access to a building can deploy an ad hoc network of snoopers and track every device in the building, with or without the approval of the building's management. The only solution is to realize that, by transmitting a packet on an 802.11 network, a mobile agent is effectively revealing its location to motivated adversaries.

6. CONCLUSION

In this paper, we presented a practical robust scheme for localization over the entirety of an 802.11 network deployed within a multi-story office building. We have shown that the use of a topological model can dramatically reduce the time required to train the localizer, while the resulting accuracy is still sufficient for many location-aware applications. We used a Gaussian fit sensor model, which is more robust and requires less training compared to sensor models that use the full histogram of signal strengths. Finally we developed a technique by which the training data can be adapted for use with totally different receiver hardware, and under different conditions than during the training phase.

To evaluate our localization technique, we have developed a methodology which makes use of excess training data to determine raw localization performance. We deployed our system in a large office building on the Rice University campus. In our experiments, we experienced both good overall performance and excellent robustness; in the rare event that an incorrect position estimate was generated, it was almost always to an adjacent cell. We also discovered how different variables, including training set size, sample size, base station density, and time of day affect localization accuracy.

Our system is ready to be made available right now in our office building for people who want to use location-aware applications on top of it, and it could be made available in the near future for deployment (after a brief training phase) in any building with an 802.11 network installed.

7. ACKNOWLEDGEMENTS

This paper has benefited considerably from the comments of the anonymous MobiCom reviewers and our shepherds, Per Gunningberg and Farooq Anjum. We would like to thank Kostas Bekris, Guillaume Marceau, and Ping Tao for contributions to earlier versions of this work. In addition, thanks to Joseph Cavallaro, Ashutosh Sabharwal, and Patrick Frantz for their insight into how wireless network cards measure signal strength. Finally, thanks to all the residents of Duncan Hall for their cooperation in our experiment, and the department chair, Keith Cooper, for trusting us with his master key.

Andreas Haeberlen is partly supported by NSF ANI-0338856 and by a fellowship from Rice University. Andrew M. Ladd is partly supported by NSF 0308237 and a FCAR Fellowship. Algis Rudys and Dan S. Wallach are supported by generous gifts from Microsoft and Schlumberger. Lydia E. Kavraki is partly supported by NSF 0308237 and a Sloan Fellowship.

8. REFERENCES

- [1] G. Abowd, K. Lyons, and K. Scott. The Rhino project, Aug. 1998. <http://www.cc.gatech.edu/fce/uvid/rhino.html>.

- [2] G. D. Abowd, C. G. Atkeson, J. Hong, S. Long, R. Kooper, and M. Pinkerton. Cyberguide: a mobile context-aware tour guide. *Wireless Networks*, 3(5):421–433, Oct. 1997.
- [3] The ACX100/ACX111 wireless network driver project. <http://acx100.sourceforge.net>.
- [4] P. Bahl and V. N. Padmanabhan. Enhancements to the RADAR user location and tracking system. Technical Report MSR-TR-2000-12, Microsoft Research, Feb. 2000.
- [5] P. Bahl and V. N. Padmanabhan. RADAR: An in-building RF-based user location and tracking system. In *Proceedings of the Nineteenth Annual Joint Conference of the IEEE Computer and Communications Societies (INFOCOM)*, volume 2, pages 775–784, Tel Aviv, Israel, Mar. 2000.
- [6] B. Brumitt, B. Meyers, J. Krumm, A. Kern, and S. Shafer. EasyLiving: Technologies for intelligent environments. In *Proceedings of the 2nd International Symposium on Handheld and Ubiquitous Computing*, Bristol, UK, Sept. 2000.
- [7] N. Bulusu, J. Heidemann, and D. Estrin. GPS-less low-cost outdoor localization for very small devices. *IEEE Personal Communications Magazine*, 7(5):28–34, Oct. 2000.
- [8] W. Burgard, A. Cremers, D. Fox, D. Hahnel, G. Lakemeyer, D. Schulz, W. Steiner, and S. Thrun. The interactive museum tour-guide robot. In *Proceedings of the Fifteenth National Conference on Artificial Intelligence (AAAI)*, Madison, WI, July 1998.
- [9] P. Castro, P. Chiu, T. Kremenek, and R. R. Muntz. A probabilistic room location service for wireless networked environments. In *Proceedings of the Third International Conference on Ubiquitous Computing (UbiComp)*, Atlanta, GA, Sept. 2001.
- [10] G. Chen and D. Kotz. A survey of context-aware mobile computing research. Technical Report TR-2000-381, Department of Computer Science, Dartmouth College, Nov. 2000.
- [11] H. Choset and K. Nagatani. Topological simultaneous localization and mapping (SLAM): Toward exact localization without explicit localization. *IEEE Transactions on Robotics and Automation*, 17(2):125–137, Apr. 2001.
- [12] I. Cox. Blanche - An experiment in guidance and navigation of an autonomous robot vehicle. *IEEE Transactions on Robotics and Automation*, 7(2):193–204, 1991.
- [13] A. K. Dey and G. D. Abowd. Cybreminder: A context-aware system for supporting reminders. In *Proceedings of the Second International Symposium on Handheld and Ubiquitous Computing*, Bristol, UK, Sept. 2000.
- [14] A. K. Dey, G. D. Abowd, and D. Salber. A context-based infrastructure for smart environments. In *Proceedings of the First International Workshop on Managing Interactions in Smart Environments*, Dublin, Ireland, Dec. 1999.
- [15] G. Dudek and M. Jenkin. *Computational Principles of Mobile Robotics*. Cambridge University Press, Cambridge, UK, 2000.
- [16] Ekahau, Inc. website. <http://www.ekahau.com/>.
- [17] Federal Communications Commission Report and Order 96-264: Revision of the commission’s rules to ensure compatibility with Enhanced 911 emergency calling systems, July 1996. <http://www.fcc.gov/Bureaus/Wireless/Orders/1996/fcc96264.txt>.
- [18] D. Fox, W. Burgard, F. Dellaert, and S. Thrun. Monte Carlo localization: Efficient position estimation for mobile robots. In *Proc. of the Sixteenth National Conference on Artificial Intelligence (AAAI-99)*, pages 343–349, Orlando, Florida, 1999.
- [19] D. Fox, W. Burgard, and S. Thrun. Markov localization for mobile robots in dynamic environments. *Journal of Artificial Intelligence Research, (JAIR)*, 11:391–427, Nov. 1999.
- [20] Y. Gwon, R. Jain, and T. Kawahara. Robust indoor location estimation of stationary and mobile users. In *Proceedings The 23rd Conference of the IEEE Communications Society (INFOCOM)*, Hong Kong, Mar. 2004.
- [21] T. He, C. Huang, B. M. Blum, J. A. Stankovic, and T. Abdelzaher. Range-free localization schemes for large scale sensor networks. In *Proceedings of the Ninth Annual International Conference on Mobile Computing and Networking (MOBICOM)*, San Diego, CA, Sept. 2003.
- [22] J. Hightower and G. Borriello. Location systems for ubiquitous computing. *IEEE Computer*, 34(8):57–66, Aug. 2001.
- [23] J. Hightower, R. Want, and G. Borriello. SpotON: An indoor 3D location sensing technology based on RF signal strength. Technical Report UW CSE 00-02-02, Department of Computer Science and Engineering, University of Washington, Seattle, WA, Feb. 2000.
- [24] J. Hill, R. Szcwzyk, A. Woo, S. Hollar, D. Culler, and K. Pister. System architecture directions for networked sensors. In *Proceedings of the Ninth International Conference on Architectural Support for Programming Languages and Operating Systems (ASPLOS-IX)*, Cambridge, MA, Nov. 2000.
- [25] L. Hu and D. Evans. Localization for mobile sensor networks. In *Proceedings of the Tenth Annual International Conference on Mobile Computing and Networking (MOBICOM)*, Philadelphia, PA, Sept. 2004.
- [26] Institute of Electrical and Electronics Engineers, Inc. *ANSI/IEEE Standard 802.11: Wireless LAN Medium Access Control (MAC) and Physical Layer (PHY) Specifications*, 1999.
- [27] C. Intanagonwiwat, R. Govindan, and D. Estrin. Directed diffusion: a scalable and robust communication paradigm for sensor networks. In *Proceedings of the Sixth Annual International Conference on Mobile Computing and Networking (MOBICOM)*, Boston, MA, Aug. 2000.
- [28] J. Krumm, S. Harris, B. Meyers, B. Brumitt, M. Hale, and S. Shafer. Multi-camera multi-person tracking for EasyLiving. In *Third IEEE International Workshop on Visual Surveillance*, Dublin, Ireland, July 2000.
- [29] J. Krumm and J. Platt. Minimizing calibration effort for an indoor 802.11 device location measurement system. Technical Report MSR-TR-2003-82, Microsoft Research, Seattle, WA, Nov. 2003.
- [30] B. Kuipers and Y.-T. Byun. A robot exploration and mapping strategy based on a semantic hierarchy of spatial representations. *Journal of Robotics and Autonomous Systems*, 8(1–2):47–63, Nov. 1991.
- [31] A. M. Ladd, K. E. Bekris, A. Rudys, G. Marceau, L. E. Kavradi, and D. S. Wallach. Robotics-based location sensing using wireless Ethernet. In *Proceedings of the Eighth Annual International Conference on Mobile Computing and Networking (MOBICOM)*, Atlanta, GA, Sept. 2002.
- [32] S. Lenser and M. Veloso. Sensor resetting localization for poorly modelled mobile robots. In *Proceedings of ICRA-2000, The International Conference on Robotics and Automation*, Detroit, MI, Apr. 2000.
- [33] T. Liu, P. Bahl, and I. Chlamtac. Mobility modeling, location tracking, and trajectory prediction in wireless ATM networks. *IEEE Journal on Selected Areas in Communications*, 16(6):922–936, Aug. 1998.

- [34] T. Logsdon. *Understanding the Navstar: GPS, GIS and IVHS. Second edition.* Van Nostrand Reinhold, New York, 1995.
- [35] N. Marmasse. comMotion: a context-aware communication system. In *CHI Extended Abstracts on Human Factors in Computing Systems*, Pittsburgh, PA, May 1999.
- [36] R. Nagpal, H. Shrobe, and J. Bachrach. Organizing a global coordinate system from local information on an ad hoc sensor network. In *Proceedings of the Second International Workshop on Information Processing in Sensor Networks (IPSN)*, Palo Alto, CA, Apr. 2003.
- [37] D. Niculescu and B. Nath. Ad hoc positioning system (APS) using AOA. In *Proceedings of the 22nd Annual Joint Conference of the IEEE Computer and Communications Societies (INFOCOM)*, San Francisco, CA, Mar. 2003.
- [38] D. Niculescu and B. Nath. DV based positioning in ad hoc networks. *Kluwer Journal of Telecommunication Systems*, 22(1-4):267–280, Jan. 2003.
- [39] G. J. Pottie and W. J. Kaiser. Wireless integrated network sensors. *Communications of the ACM*, 43(5):51–58, May 2000.
- [40] N. Priyantha, A. Chakraborty, and H. Balakrishman. The Cricket location support system. In *Proceedings of the Sixth Annual International Conference on Mobile Computing and Networking (MOBICOM)*, pages 32–43, Boston, MA, Aug. 2000.
- [41] N. Priyantha, A. Miu, H. Balakrishman, and S. Teller. The Cricket Compass for context-aware mobile applications. In *Proceedings of the Seventh Annual International Conference on Mobile Computing and Networking (MOBICOM)*, pages 1–14, Rome, Italy, July 2001.
- [42] E. Remolina and B. Kuijpers. Towards a general theory of topological maps. *Artificial Intelligence*, 152(1):47–104, Jan. 2004.
- [43] T. Roos, P. Myllymaki, H. Tirri, P. Misikangas, and J. Sievanan. A probabilistic approach to WLAN user location estimation. *International Journal of Wireless Information Networks*, 9(3), July 2002.
- [44] A. Savvides, C.-C. Han, and M. B. Strivastava. Dynamic fine-grained localization in ad-hoc networks of sensors. In *Proceedings of the Seventh Annual International Conference on Mobile Computing and Networking (MOBICOM)*, Rome, Italy, July 2001.
- [45] A. Smailagic, D. Siewiorek, J. Anhalt, D. Kogan, and Y. Wang. Location sensing and privacy in a context aware computing environment. *Pervasive Computing*, 2001.
- [46] J. Small, A. Smailagic, and D. P. Siewiorek. Determining user location for context aware computing through the use of a wireless LAN infrastructure, Dec. 2000. <http://www-2.cs.cmu.edu/~aura/docdir/small00.pdf>.
- [47] C. Steger, P. Radosavljevic, and P. Frantz. 802.11b operating in a mobile channel: Performance and challenges. In *Communications Design Conference*, San Jose, CA, Sept. 2003.
- [48] P. Tao, A. Rudys, A. M. Ladd, and D. S. Wallach. Wireless LAN location-sensing for security applications. In *Proceedings of the Second ACM Workshop on Wireless Security (WiSe)*, San Diego, CA, Sept. 2003.
- [49] S. Thrun. Probabilistic algorithms in robotics. *AI Magazine*, 21(4):93–109, 2000.
- [50] S. Thrun and A. Bücken. Integrating grid-based and topological maps for mobile robot navigation. In *Proceedings of the AAAI Thirteenth National Conference on Artificial Intelligence*, Portland, Oregon, Aug. 1996.
- [51] S. Thrun and A. Bücken. Learning maps for indoor mobile robot navigation. Technical Report CMU-CS-96-121, Carnegie Mellon University, Computer Science Department, Pittsburgh, PA, Apr. 1996.
- [52] S. Thrun, W. Burgard, and D. Fox. A probabilistic approach to concurrent mapping and localization for mobile robots. *Machine Learning*, 31(1-3):29–53, 1998.
- [53] S. Thrun, D. Fox, W. Burgard, and F. Dellaert. Robust Monte Carlo localization for mobile robots. *Artificial Intelligence*, 101:99–141, 2000.
- [54] S. Thrun, J.-S. Gutmann, D. Fox, W. Burgard, and B. Kuijpers. Integrating topological and metric maps for mobile robot navigation: A statistical approach. In *Proceedings of the Fifteenth National Conference on Artificial Intelligence and Tenth Conference on Innovative Applications of Artificial Intelligence*, pages 989–995, Madison, WI, July 1998.
- [55] R. Want, A. Hopper, V. Falco, and J. Gibbons. The Active Badge location system. *ACM Transactions on Information Systems*, 10:91–102, Jan. 1992.
- [56] A. Ward, A. Jones, and A. Hopper. A new location technique for the active office. *IEEE Personal Communications*, 4(5):42–47, Oct. 1997.
- [57] R. Yamamoto, H. Matsutani, H. Matsuki, T. Oono, and H. Ohtsuka. Position location technologies using signal strength in cellular systems. In *Proc. of the 53rd IEEE Vehicular Technology Conference*, Rhodes, Greece, May 2001.
- [58] M. Youssef, A. Agrawala, and A. U. Shankar. WLAN location determination via clustering and probability distributions. In *Proceedings of the IEEE International Conference on Pervasive Computing and Communications (PerCom)*, Fort Worth, TX, Mar. 2003.

APPENDIX

A. PRACTICAL EXPERIENCE

During our large-scale experiment, we learned several practical lessons that we believe to be relevant when validating our results or deploying the system in another building.

First of all, it is essential to avoid time-varying effects when collecting the training set; otherwise there may be inconsistencies between different parts of the building or even between adjacent cells. We gathered most of our training data in two consecutive nights during spring break, when the building was empty.

Second, entering all the rooms in a building raises privacy and trust issues. Before we obtained a master key, we notified all the residents of the building and gave them an opportunity to object, or to be present during the experiment. Also, we found that there were some rooms (such as the dean’s office) that even the official master key did not open.

Third, battery capacity and notebook weight are limiting factors. Even a light notebook is impossible to carry with outstretched arms for an extended period of time. Also, constantly sending radio signals tends to drain batteries very quickly.

Finally, in gathering the training data, we were continually reminded that we were essentially violating the personal space of the occupants of our building. Offices contained such obscure items as a paper skeleton and a complete knight’s armor. We were also exposed to the tendency of some occupants of our building to not bathe or dispose of spoiled foods.